analytical chemistry

ACS AuthorChoice

Article

pubs.acs.org/ac

Terms of Use

Mobility-Resolved Ion Selection in Uniform Drift Field Ion Mobility Spectrometry/Mass Spectrometry: Dynamic Switching in Structures for Lossless Ion Manipulations

Ian K. Webb, Sandilya V. B. Garimella, Aleksey V. Tolmachev, Tsung-Chi Chen, Xinyu Zhang, Jonathan T. Cox, Randolph V. Norheim, Spencer A. Prost, Brian LaMarche, Gordon A. Anderson, Yehia M. Ibrahim, and Richard D. Smith*

Biological Sciences Division and Environmental Molecular Sciences Laboratory, Pacific Northwest National Laboratory, 3335 Innovation Avenue (K8-98), P.O. Box 999, Richland, Washington 99352, United States

ABSTRACT: A Structures for Lossless Ion Manipulations (SLIM) module that allows ion mobility separations and the switching of ions between alternative drift paths is described. The SLIM switch component has a "Tee" configuration and allows the efficient switching of ions between a linear path and a 90-degree bend. By controlling switching times, ions can be efficiently directed to an alternative channel as a function of their mobilities. In the initial evaluation the switch is used in a static mode and shown compatible with high performance ion mobility separations at 4 Torr. In the dynamic mode, we show that mobility-selected ions can be switched into the alternative channel, and that various ion species can be independently selected based on their mobilities for time-of-flight mass spectrometer (TOF MS) IMS detection and mass analysis. This development also provides the basis of, for example, the selection of specific mobilities for storage and accumulation, and the key component of modules for the assembly of SLIM devices enabling much more complex sequences of ion manipulations.

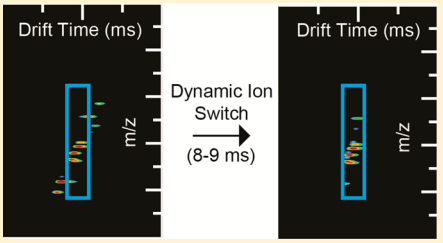

Ion mobility spectrometry/mass spectrometry (IMS/MS) is a technique that separates ions based on their size-to-charge and mass-to-charge (m/z) ratios, respectively.[1] IMS/MS has been applied for ion separations of compounds from complex mixtures,[2] including, for example, peptides,[3] proteins,[4] lipids,[5] carbohydrates,[6] and tissue samples.[7] IMS/MS has also been applied to the separation of structural isomers,[8] for example, protein conformers.[9] There are several types of IMS instruments widely used for biomolecular analysis, including low-field drift tube IMS[10,11] and high-field asymmetric ion mobility spectrometry (FAIMS).[12] Low-field drift tube instruments operate by allowing ions to traverse through the drift tube by means of DC potentials in the presence of a buffer gas, with drift motion governed by diffusion. Ions are introduced by gated pulses, conventionally via a Bradbury–Nielsen gate,[13] into the drift tube to establish an initial time to separate ions by their drift times. More recently, for greater ion duty cycle and sensitivity, gating[14] and trapping[15] (as well as ion accumulation) in ion funnels have been employed to pulse ions into the IMS. Additionally, ion utilization efficiency from continuous ion sources can be increased by multiplexing ion pulsing events.[16−18] Ion mobilities (K) can be directly measured for each ion from drift tube IMS by the following equation

$$K = \frac{L}{t_d E}$$

where L is the drift tube length, t_d is the ion drift time, and E is the electric field across the drift tube. Collisional cross sections of ions can be calculated by the Mason equation[19]

$$\Omega = \frac{3ez}{16N}\left(\frac{2\pi}{\mu kT}\right)^{1/2}\frac{1}{K}$$

where N is the number density of the buffer gas, μ is reduced mass of the ion and buffer gas, T is temperature, and Ω is the measured collisional cross section. Measured cross sections can be compared to theoretical cross section approximations[20,21] or experimentally determined NMR or X-ray diffraction structures to gain insight into gas-phase 3-D structural information.[22]

The mobility selection of ions has been previously achieved using FAIMS,[23] differential mobility analyzers (DMA),[24] overtone mobility spectrometry (OMS),[25] and double gated low field drift tube IMS[26] devices for applications. FAIMS utilizes the differences in mobilities at high versus low electric fields by applying a high electric field for a short time and a low electric field for a comparatively longer time, such that the times the fields are applied are asymmetric. Ions eventually collide with the electrodes unless a compensation voltage (CV) is used to select a specific high field to low field mobility ratio to pass through the device. By scanning the CV, an ion mobility spectrum can be obtained, but with either very low resolving

Received: June 10, 2014
Accepted: September 15, 2014
Published: September 15, 2014

   dx.doi.org/10.1021/ac502139e | *Anal. Chem.* 2014, 86, 9632−9637

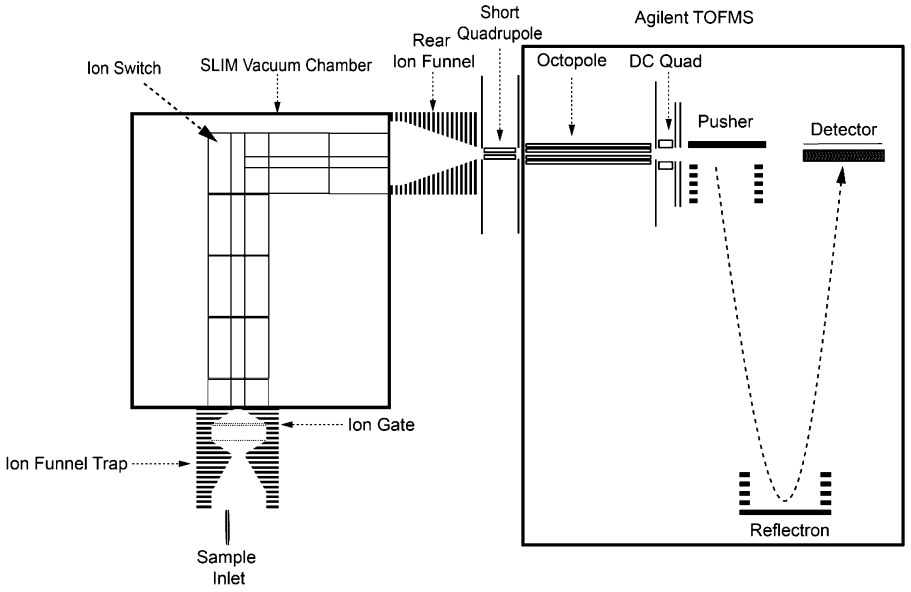

Figure 1. Schematic of SLIM/TOF MS arrangement used in this work, including the SLIM ion switch component. Ions must be switched 90° from their original drift trajectory to be detected by the TOF MS.

power or very low transmission efficiency (and hence significantly reduced sensitivity).[27] In DMA charged particles, especially aerosols or nanoparticles, travel in a gas flow perpendicular to the ion drift motion between two plates with a potential applied between the two plates. Mobility selection occurs by scanning the applied potential such that ions of specific mobilities pass through a slit to a particle counter, where the ions are dispersed in space by size, but provides sensitivities constrained by the limited size of the both the entrance and sampling slits if reasonable resolutions are to be achieved, as well as low transmission efficiency because of loss of ions with mobilities other than the mobility selected by the applied potential. The overtone mobility approach uses an arrangement that is similar to conventional drift tube instruments, but is operated by changing the electric fields in specific drift regions at a certain frequency that selects a small range of mobilities that can travel through the device. Ions also have stable trajectories at the overtones of the selected frequencies, with increasing resolving power for the higher order overtones. Finally, ions can be selected in a low electric field drift tube using an ion gate after the drift tube, allowing only ions selected by their mobilities (i.e., during the gate "open" period) to pass to the detector. While this approach does not impact sensitivity, information for the rest of the separation is lost.

Recently, structures for lossless ion manipulations (SLIM) have been introduced and characterized with both simulations and measurements, and shown to provide the basis for effectively lossless ion transmission, for example, at 4 Torr and over a significant m/z range.[28−30] IMS separations in SLIM have been shown to achieve near theoretical limits of resolving power.[30,31] A key interest with SLIM is the assembly of simple components, initially being constructed from 7.62 × 7.62 cm printed circuit boards, into more complex modules that enable a range of functionalities, and then can be assembled into even more complex devices. The initial devices have been shown to efficiently transmits ions of mass <180 to >2700 m/z.[29,30] Key SLIM components include straight and 90° turning ion drift segments that, for example, can be assembled into IMS modules by different arrangements of the individual components. In this work, the dynamic ion switch component is introduced. The ion switch can be operated in modes that either selects ions by their mobilities for direction to an orthogonal channel as they arrive in the switching region (dynamic mode) or to allow all ions to pass for continued drift in a linear channel (static mode). By coupling the ion switch with other SLIM components, a low field drift IMS module has been constructed with the ability to select ions by mobility, allowing new flexibility for IMS/MS applications.

EXPERIMENTAL ARRANGEMENT

ESI-SLIM/MS. Agilent Low Concentration Tuning Mix (Agilent, Santa Clara, CA) and a mixture of 9 peptides infused at a flow rate of 300 nL/min to the ESI source were used to demonstrate the capabilities of the SLIM ion switch component and its respective IMS module. The 9 peptide mix was an equimolar mixture of 1 μM of each bradykinin acetate salt, kemptide acetate salt, angiotensin I human acetate salt hydrate, angiotensin II human, neurotensin, renin substrate tetradecapeptide porcine, substance P acetate salt hydrate, melittin from honey bee venom, and fibrinopeptide A human (Sigma-Aldrich, St. Louis, MO). The mixture solvent was composed of 50/50/1 vol/vol/vol water/methanol/acetic acid (Fisher Scientific, Pittsburgh, PA). The TOF MS system, and its modifications for SLIM evaluation as used in this study has been described in detail elsewhere (Figure 1).[30] Briefly, ions are introduced from a nanoelectrospray (2300 V) source into an ion funnel trap[15,32] (3.95 Torr) where ions are stored and gated for 486 μs into the SLIM. The SLIM module (at 4.00 Torr) was comprised of one 3.05 cm linear, three 7.62 cm linear, a switch, and two additional 7.62 cm linear components positioned such that ions were switched orthogonally to their original path (Figure 1). Each component comprises two SLIM surfaces spaced ∼5 mm apart in this work. Each SLIM component PCB incorporates a central array of "rung" RF electrodes operated 180° out of phase with each neighboring electrode. The rungs are bordered on either side by DC-only "guard" electrodes that provide lateral ion confinement. Ions exiting the SLIM module are

dx.doi.org/10.1021/ac502139e | Anal. Chem. 2014, 86, 9632−9637

efficiently transmitted by a rear ion funnel to a region containing a short quadrupole at 475 mTorr for transmission to an Agilent 6224 TOF MS with a 1.5 m flight tube (Agilent, Santa Clara, CA). In this work the SLIM module was operated with an axial 14 V/cm DC uniform drift field with an 11 V DC guard bias (Figure 2) and a 650 kHz, 320 V_{p-p} RF waveform was applied for all experiments.

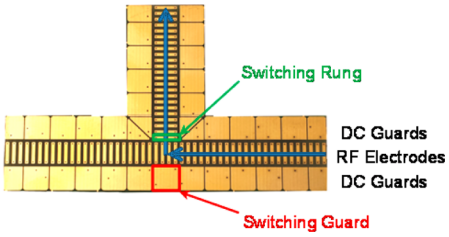

Figure 2. Schematic of the RF and guard electrodes on the dynamic ion switch component. The switching guard voltage is raised by 100 V to direct the ions orthogonal to their original drift path.

SLIM Dynamic Switch Operation. The electrode configuration for the dynamic ion switch component is shown in Figure 2. Ions drift from the ion funnel trap to the switch where they either (i) continue on a straight path (switch off) or (ii) switched to an orthogonal path (switch on) for TOF MS detection. The switching guard electrode denoted in Figure 2 was independently controlled so that its DC voltage could be raised to switch ions to the orthogonal path or lowered to allow ions to continue along the straight path. The DC voltage on the switching rung in the orthogonal ion path was also switched to a higher potential to confine ions for continued travel in the straight path, or to a lower potential to switch ions into the orthogonal path. The switching of these two electrodes was synchronized. The switching rung was the first electrode of the DC gradient along the orthogonal ion path. Adjusting the switching rung voltage did not affect any voltages on the rung electrodes of the original straight path, but did affect the voltages in the orthogonal path. When the switch was turned on, the switching rung was biased such that an average 14 V/cm gradient is maintained along the entire orthogonal path. The voltage on the switching guard was set to 543 V to allow ions to travel through the straight path, while the switch is off. The switching rung was biased 10 V DC lower than the switching guard voltage to prevent ion loss in the orthogonal direction. The switching guard electrode was raised an additional 100 to 643 V and the switching rung was lowered by 5 V DC to 528 V to turn the switch on. Ion trajectory simulations showed this voltage profile yields lossless ion transmission in either of the two directions.[29] These voltages were controlled by power supplies triggered by the opening of the exit ion gate in the ion funnel trap, where time delays and pulse widths can be controlled using in-house developed instrument control

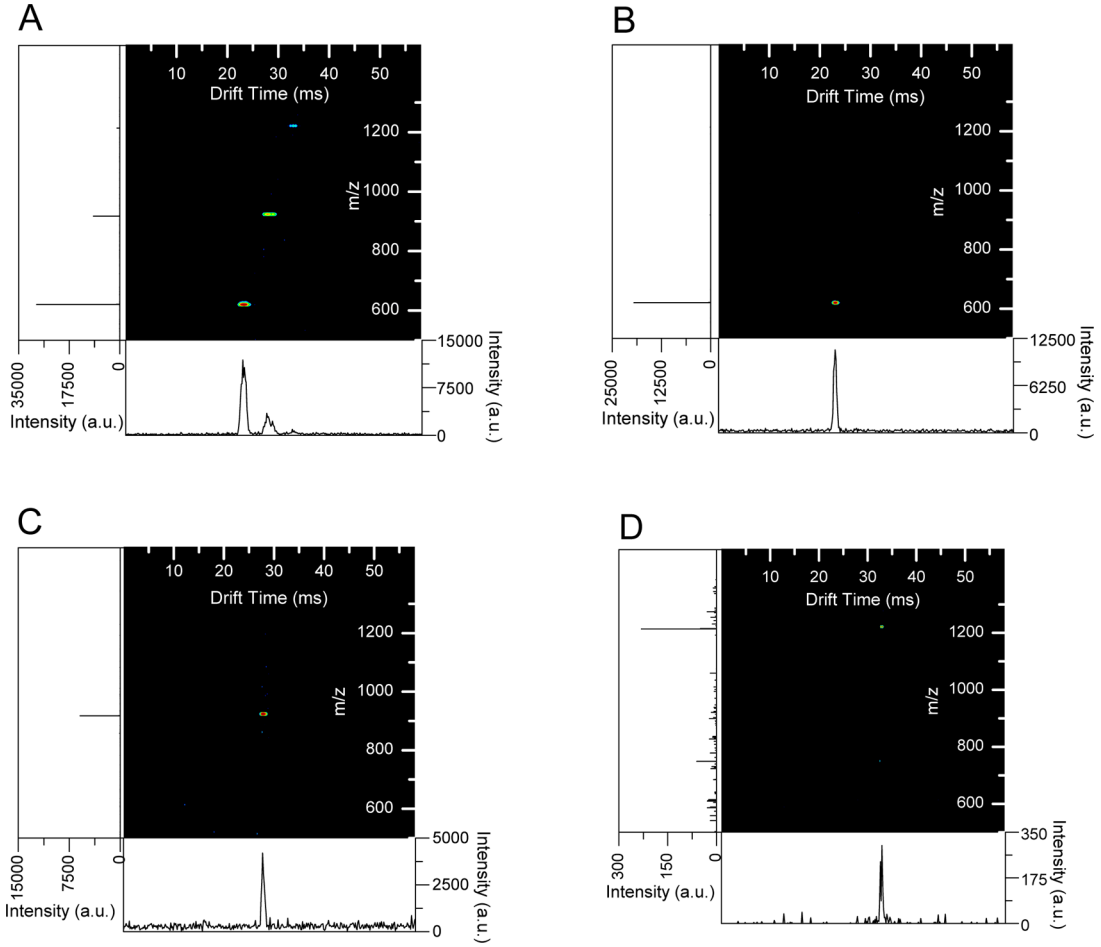

Figure 3. Comparison of IMS/MS spectra resulting from operating the switch in either static mode (a) or dynamic mode (b–d). (b) Ions switched from 10.50 to 11.31 ms. (c) Ions switched from 13.3 to 14.11 ms. (d) Ions switched from 16.25 to 17.06 ms.

dx.doi.org/10.1021/ac502139e | Anal. Chem. 2014, 86, 9632–9637

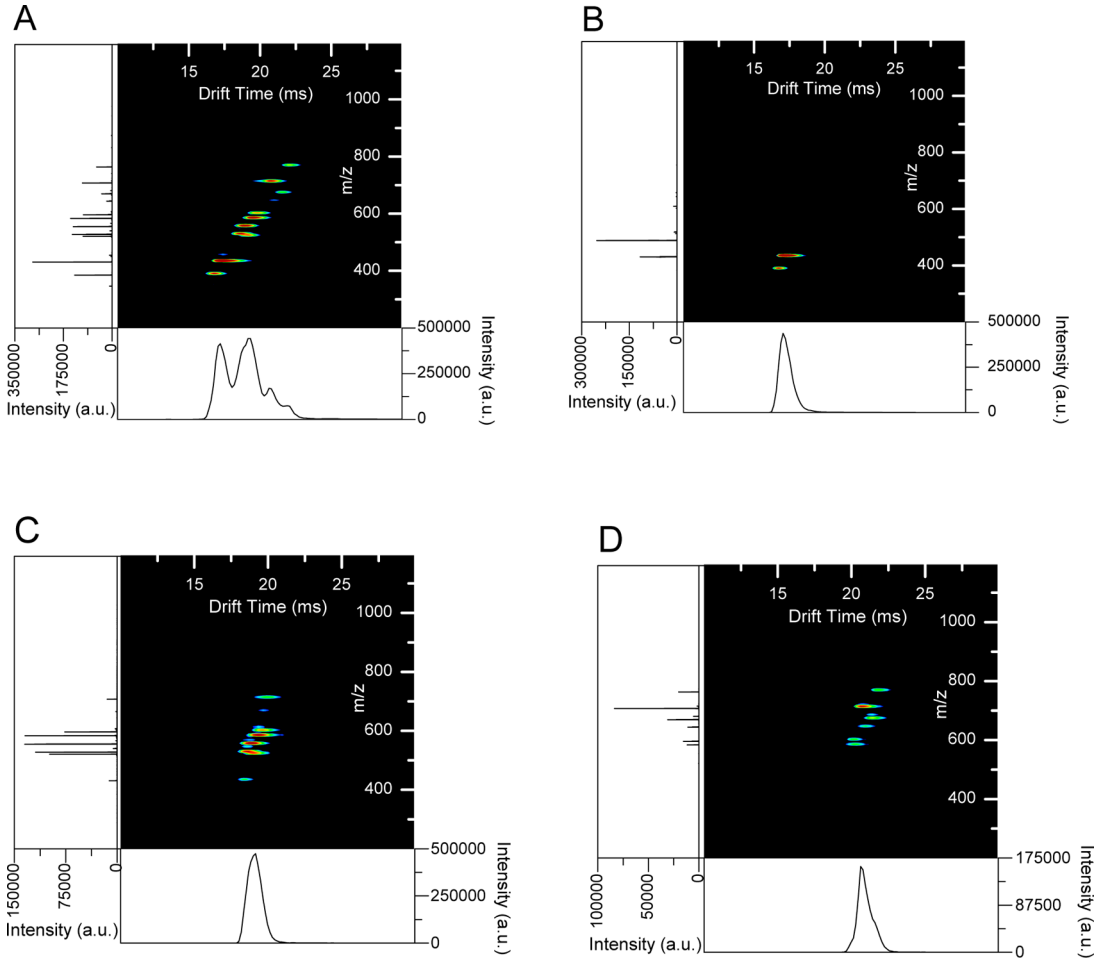

Figure 4. Selection of IMS features from 9 peptide mix with the dynamic ion switch. (a) Switch is in static mode to obtain complete IMS spectrum. (b) Dynamic switching for 7.00−8.00 ms. (c) Dynamic switching for 8.00−9.00 ms. (d) Dynamic switching for 9.00−10.00 ms.

software. Rise times for the switching guard voltage were measured to be on the order of ∼140 μs, allowing for mobility-resolved ion selection.

RESULTS AND DISCUSSION

Demonstration of IMS and Mobility-Resolved Ion Selection. To initially evaluate the capabilities of the SLIM dynamic ion switch component, ions were transferred through the SLIM module in static and dynamic switching modes. In static mode, the necessary voltages to move ions into the orthogonal path (+100 V bias on the switching guard, DC bias of switching rung lowered 5 V) are constantly applied. This mode allows for the collection of conventional drift IMS/MS spectra (Figure 3a) similar to the 90° turn investigated in previous work.[29,30] Dynamic mode switching was used to select individual ion species by their mobilities and switch them into the orthogonal path to the MS (Figure 3b−d). Ions that were not switched (or selected) continued to move in the straight path. In the dynamic mode, the switch was on only for 0.81 ms. For Figure 3b, the switch was turned on from the time period of 10.50 to 11.31 ms after the ions were released from the ion funnel trap (i.e., t_0). Only ions from the first IMS peak (m/z 622) were switched to the mass spectrometer in this 0.81 ms switch on pulse. The ion clouds for m/z 922 and 1222 were not observed, as they reached the switch after it had been turned off. The dynamic switching sequence was repeated for m/z 922 (Figure 3c), with the switch on from 13.30 to 14.11 ms after t_0, and for m/z 1222 (Figure 3d), from 16.25 to 17.06 ms after t_0. All three selected IMS/MS spectra (Figure 3b−3d) show only the specific peak that was chosen without cross contamination from peaks of other mobilities.

Selection of IMS Features from a Peptide Mixture. The dynamic ion switch was used to select specific mobility features from the IMS spectrum of the 9 peptide mix. The switch was operated in static mode to obtain the complete IMS spectrum (Figure 4a). The resulting IMS spectrum shows that there are at least 3 features in the IMS spectrum, including features with arrival times of 17.24, 19.09, 20.75 ms (the shoulder on 19.09 ms). Peaks with IMS arrival times within the first feature were switched in Figure 4b by switching from 7.00 to 8.00 ms after t_0. The resulting ions were m/z 387 (kemptide, $[M + 2H]^{2+}$) and 433 (angiotensin I, $[M + 3H]^{3+}$), which both have arrival times within the first IMS feature. The second and third features are no longer present in the IMS/MS spectrum. Ions in the second IMS feature were selected by switching ions arriving at the switch from 8.00 to 9.00 ms after t_0. The observed peptide ions in this case were m/z 524 (angiotensin II $[M + 2H]^{2+}$), 531 (bradykinin $[M + 2H]^{2+}$), 558 (neurotensin $[M + 3H]^{3+}$), and 587 (renin substrate tetradecapeptide $[M + 3H]^{3+}$), also including the tails of m/z 433 and 712 (melittin $[M + 4H]^{4+}$) IMS peaks. Each of the peptide ions switched are within the bounds of the second IMS feature in Figure 4a, while the two peaks that tail into the IMS spectrum in Figure 4c can

dx.doi.org/10.1021/ac502139e | Anal. Chem. 2014, 86, 9632−9637

be seen to be tailing into the second IMS feature in the full spectrum (Figure 4a). The switching experiment was performed again for 9.00−10.00 ms after t_0 (Figure 4d), switching peptide ions at m/z 675 (substance P $[M + 2H]^{2+}$), 712, and 769 (fibrinopeptide A $[M + 2H]^{2+}$), as well as the shoulders of peptide ions m/z 587 and 649 (angiotensin I $[M + 2H]^{2+}$). Again, the peptide ions appear within the selected mobility feature in Figure 4a as well, and m/z 587 and 649 are tailing into the third mobility feature, resulting in this population of ions being switched to the mass spectrometer.

Though each of the previous cases shows selection of a single mobility window at a time, there is no inherent restriction to operating the switch in this fashion. The dynamic ion switch allows for mobility ion selection of multiple mobility windows (Figure 5). The 9 peptide mix ions were switched from 7.00 to

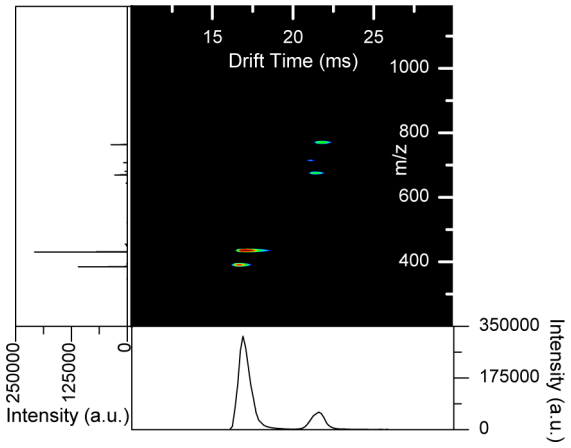

Figure 5. Multiple ion switching events within a single mobility separation. Nine peptide mix switched at 7.00−7.50 and 9.50−10.00 ms after t_0.

7.50 ms (IMS peak at arrival time 16.98 ms) and 9.50 to 10.00 ms (IMS peak at arrival time 21.57 ms). Again, the peaks that overlap these regions in Figure 4a are the peaks that were switched; however, both regions are switched within a single IMS experiment.

CONCLUSION

A SLIM dynamic ion switch component has been demonstrated to provide ion transmission through an orthogonal path and to provide ion selection based upon mobility. The dynamic ion switch allows for mobility selection in conjunction with field drift ion mobility separations. It has previously been shown that SLIM IMS performance is close to theoretical and with results obtained from conventional drift tube designs. In this work we have shown that high quality IMS/MS performance can also obtained with the switch in static mode, and also in conjunction with ion selection, that is, using the switch in a dynamic (mobility-resolved) mode. Specific mobilities can be selected if there is sufficient IMS separation prior to the switch segment, as demonstrated by selective isolation of m/z 622, 922, and 1222 ions from a simple mixture. In addition, the ability to select mobility features from a mixture of peptides and select multiple mobility windows in a single mobility separation was demonstrated. The development and demonstration of the SLIM ion switch component and the simple IMS module provides a foundation for the assembly of much more complex SLIM modules or devices that, for example, switch ions into storage and accumulation trapping or reaction regions, and after which further mobility separations can be conducted. The present work also demonstrates the key components that will be required for the assembly of a multipass "mobility cyclotron" module with the potential to enable extremely high resolving power separations.[33,34]

The SLIM switch component offers many advantages over existing ion selection technology. The ion switch can be physically implemented multiple times within a single SLIM module or device, owing to its small size and flexibility. For the OMS and gated drift cell approaches, this is much more difficult due to the resulting size and cost of such a hypothetical instrument. In addition, it is possible for the ions that are not switched to continue on to a different path for additional analysis and not be inherently lost as they are for the OMS and dual gated drift cell approaches. The small size and flexibility of coupling mobility selection capabilities to SLIM modules and devices using the SLIM switch provides the basis for much more complicated ion manipulations than using the currently available platforms.

AUTHOR INFORMATION

Corresponding Author

*E-mail: rds@pnnl.gov.

Notes

The authors declare no competing financial interest.

ACKNOWLEDGMENTS

Portions of this research were supported by the National Institutes of Health (NIH) NIGMS grant P41 GM103493, the U.S. DOE Office of Biological and Environmental Research Pan-omics program at PNNL, and the Laboratory Directed Research and Development (LDRD) program at Pacific Northwest National Laboratory. Work was performed in the Environmental Molecular Science Laboratory, a U.S. Department of Energy (DOE) national scientific user facility at Pacific Northwest National Laboratory (PNNL) in Richland, WA. PNNL is operated by Battelle for the DOE under contract DE-AC05-76RL0 1830.

REFERENCES

(1) Kanu, A. B.; Dwivedi, P.; Tam, M.; Matz, L.; Hill, H. H. *J. Mass Spectrom.* **2008**, *43*, 1.
(2) Bohrer, B. C.; Mererbloom, S. I.; Koeniger, S. L.; Hilderbrand, A. E.; Clemmer, D. E. *Annu. Rev. Anal. Chem.* **2008**, *1*, 293.
(3) Hoaglund-Hyzer, C. S.; Clemmer, D. E. *Anal. Chem.* **2001**, *73*, 177.
(4) Sowell, R. A.; Koeniger, S. L.; Valentine, S. J.; Moon, M. H.; Clemmer, D. E. *J. Am. Soc. Mass Spectrom.* **2004**, *15*, 1341.
(5) Kliman, M.; May, J. C.; McLean, J. A. *Biochim. Biophys. Acta, Mol. Cell Biol. Lipids* **2011**, *1811*, 935.
(6) Dwivedi, P.; Bendiak, B.; Clowers, B.; Hill, H. H. *J. Am. Soc. Mass Spectrom.* **2007**, *18*, 1163.
(7) Ridenour, W. B.; Kliman, M.; McLean, J. A.; Caprioli, R. M. *Anal. Chem.* **2010**, *82*, 1881.
(8) Wu, C.; Siems, W. F.; Klasmeier, J.; Hill, H. H. *Anal. Chem.* **2000**, *72*, 391.
(9) Clemmer, D. E.; Hudgins, R. R.; Jarrold, M. F. *J. Am. Chem. Soc.* **1995**, *117*, 10141.
(10) Wu, C.; Siems, W. F.; Asbury, G. R.; Hill, H. H. *Anal. Chem.* **1998**, *70*, 4929.
(11) Bowers, M. T. *Int. J. Mass Spectrom.* **2014**, *370*, 75.
(12) Purves, R. W.; Guevremont, R. *Anal. Chem.* **1999**, *71*, 2346.

(13) Yoon, O. K.; Zuleta, I. A.; Robbins, M. D.; Barbula, G. K.; Zare, R. N. *J. Am. Soc. Mass Spectrom.* **2007**, *18*, 1901.
(14) Tang, K.; Shvartsburg, A. A.; Lee, H. N.; Prior, D. C.; Buschbach, M. A.; Li, F. M.; Tolmachev, A. V.; Anderson, G. A.; Smith, R. D. *Anal. Chem.* **2005**, *77*, 3330.
(15) Clowers, B. H.; Ibrahim, Y. M.; Prior, D. C.; Danielson, W. F., III; Belov, M. E.; Smith, R. D. *Anal. Chem.* **2008**, *80*, 612.
(16) Clowers, B. H.; Siems, W. F.; Hill, H. H.; Massick, S. M. *Anal. Chem.* **2006**, *78*, 44.
(17) Belov, M. E.; Buschbach, M. A.; Prior, D. C.; Tang, K.; Smith, R. D. *Anal. Chem.* **2007**, *79*, 2451.
(18) Belov, M. E.; Clowers, B. H.; Prior, D. C.; Danielson, W. F., III; Liyu, A. V.; Petritis, B. O.; Smith, R. D. *Anal. Chem.* **2008**, *80*, 5873.
(19) Revercomb, H. E.; Mason, E. A. *Anal. Chem.* **1975**, *47*, 970.
(20) von Helden, G.; Hsu, M. T.; Gotts, N.; Bowers, M. T. *J. Phys. Chem.* **1993**, *97*, 8182.
(21) Shvartsburg, A. A.; Jarrold, M. F. *Chem. Phys. Lett.* **1996**, *261*, 86.
(22) Creaser, C. S.; Griffiths, J. R.; Bramwell, C. J.; Noreen, S.; Hill, C. A.; Thomas, C. L. P. *Analyst* **2004**, *129*, 984.
(23) Kolakowski, B. M.; Mester, Z. *Analyst* **2007**, *132*, 842.
(24) Guha, S.; Li, M.; Tarlov, M. J.; Zachariah, M. R. *Trends Biotechnol.* **2012**, *30*, 291.
(25) Kurulugama, R. T.; Nachtigall, F. M.; Valentine, S. J.; Clemmer, D. E. *J. Am. Soc. Mass Spectrom.* **2011**, *22*, 2049.
(26) Clowers, B. H.; Hill, H. H. *Anal. Chem.* **2005**, *77*, 5877.
(27) Shvartsburg, A. A.; Creese, A. J.; Smith, R. D.; Cooper, H. J. *Anal. Chem.* **2010**, *82*, 8327.
(28) Tolmachev, A. V.; Webb, I. K.; Ibrahim, Y. M.; Garimella, S. V. B.; Zhang, X.; Anderson, G. A.; Smith, R. D. *Anal. Chem.* **2014**, *86* (18), 9162−9168.
(29) Garimella, S. V. B.; Ibrahim, Y. M.; Webb, I. K.; Tolmachev, A. V.; Zhang, X.; Prost, S. A.; Anderson, G. A.; Smith, R. D. *J. Am. Soc. Mass Spectrom.* **2014**, in press.
(30) Webb, I. K.; Garimella, S. V. B.; Tolmachev, A. V.; Chen, T. C.; Zhang, X.; Norheim, R. V.; Prost, S. A.; LaMarche, B. L.; Anderson, G. A.; Ibrahim, Y. M.; Smith, R. D. *Anal. Chem.* **2014**, *86*, 9169.
(31) Siems, W. F.; Wu, C.; Tarver, E. E.; Hill, H. H.; Larsen, P. R.; McMinn, D. G. *Anal. Chem.* **1994**, *66*, 4195.
(32) Ibrahim, Y.; Belov, M. E.; Tolmachev, A. V.; Prior, D. C.; Smith, R. D. *Anal. Chem.* **2007**, *79*, 7845.
(33) Merenbloom, S. I.; Glaskin, R. S.; Henson, Z. B.; Clemmer, D. E. *Anal. Chem.* **2009**, *81*, 1482.
(34) Glaskin, R. S.; Valentine, S. J.; Clemmer, D. E. *Anal. Chem.* **2010**, *82*, 8266.

dx.doi.org/10.1021/ac502139e | *Anal. Chem.* 2014, 86, 9632−9637